

## Human Eye Response to Pupil Size Variation Programmatically

Zaher Ataa Naeem<sup>a</sup>, Ahmed Luay Ahmed<sup>b</sup>, Rajaa Ahmed Ali<sup>c</sup>

<sup>a</sup>Ministry of Education, Al Resafal Education Directorate, Iraq.

<sup>b</sup>Ministry of Higher Education and Scientific Research, Iraq

<sup>c</sup>Computer Science Department, College of Science, University of Diyala, Iraq

**Article History:** Received: 11 January 2021; Revised: 12 February 2021; Accepted: 27 March 2021; Published online: 16 April 2021

**Abstract:** The human eye is the best optical device in the world. The performance of this eye is influenced by optical aberrations. Several human eye models were developed to treat and correct this issue. To build and study the optimal and berated human eye, this work relies on the Liou and Brennan eye model. This model is more suitable than other models since it depends on using a gradient refractive index ( $n$ ) with a spherical lens surface. The effect of entrance pupil diameter on optical aberrations were evaluated programmatically by ZEMAX , computer software (version 14) at 555 nm monochromatic light under the influence of Semi-Diameter values variation by 1.25, 1.5, 2, 3, 4 and 5 mm. The eye's performance was evaluated using the modulation transfer function (MTF), root mean square of the spot sizes (RMS), and wave front aberration. The findings showed that the best image quality acquired at 1.25 and 1.5mm Semi-diameter, which means that under monochromatic illumination, the smallest values of aberrations can be obtained by using a small pupil scale and a small field of view.

**Keywords:** Human Eye, Pupil Size, Field of View, Intraocular Lens.

### 1. Introduction

The human eye is an interesting optical instrument. The principles of picture forming by the eye are identical with the manufactured optical systems (Artal 2015). Light reaches the eye from the cornea, which is afterwards refracted by the cornea and lens, to be focused at the retina (Burns et al. 2019). The cornea with refractive index 1.376 also has a greater power than the lens. However, the corneal power is constant and its optical properties can be altered according to diseases affecting the cornea (Polans et al. 2015); the power of the lens is changeable, and it alters while the eye demands to focus at varying ranges. The iris, which is the colored part of the eye and the pupil (the iris opening) control the incoming light beam diameter and it forms the eye stop aperture. The aperture stop, like all optical devices, is a critical aspect that affects a broad variety of optical processes (Atchison & Thibos 2016). The appearance of the eye is similar to a spherical ball. The geometry of the human eye is seen in Figure (1), and the most important optical data are mentioned in Table (1). For objects at infinity, the relaxed eye is distinguished from the suited or focused status (Kaschke et al. 2013).

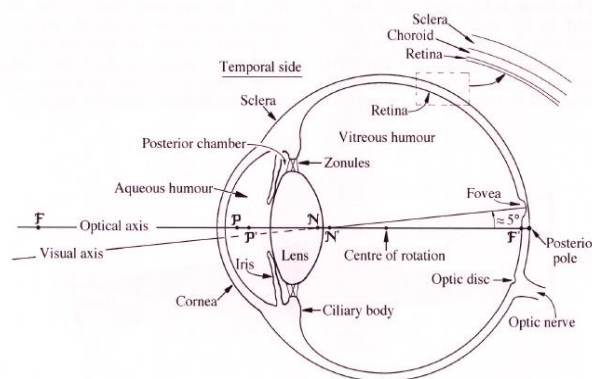


Figure 1. Details and geometry of the human eye (D. Atchison & Smith 2000).

Table 1. The human eye's major optical parameters

Property	Relaxed	Accommodated
Power of refractive	58.63 D	70.57 D
Focal length in air	17.1 mm	14.2 mm

The crystalline lens's refractive strength	19 D	33 D
Maximum field of view	108°	
Field of view – fovea	5°	
Diameter of the pupil	2–8 mm	
F-number	6.8–2.4	
The eyeball's diameter	24 mm	
The front vertex's distance from the rotation point	13.5 mm	
Wavelength of largest sensitivity	555 nm	
The front vertex's distance from the nodal point N	7.33 mm	
The front vertex's distance from the principal plane P	1.6 mm	
The front vertex's distance from the entrance pupil	3.0 mm	

## 2. Optical Aberrations

As an optical system, the human eye; focuses the incoming light by its optical components to form the image onto the retina (Bartuzel et al. 2019). The deviation of the light from its direction may be caused by imperfections in these components. Optical aberrations are those deviations that result in image blurring and visual performance decreasing (Cholewiak et al. 2018). Optical aberrations are affected by several kinds of aberrations such as:

- Spherical aberration (SA): It is observed in optical devices that occur due to the increased refraction of light (Batres et al. 2020), where the non-spherical surfaces are free of SA (Miks & Novak,2016). The correction of SA can be done by changing the lens shape or pleating the lens, to reduce (Vukobratovich & Yoder 2018).
- Coma aberration: is the most noticeable when looking away from the visual axis (at small field angles) (Miks & Novak,2016), in a thin lens it depends on its position and shape factor (Mahajan, 2011).
- Astigmatism: When the beam from an off-axis object converges on two diverse image planes, this occurs (Nakajima 2015).
- Distortion aberration: When an off-axis point's image is shaped further from the axis or closer to the axis than the image height, it is said to be that the image of the extended origin is distorted (Smith 2007).
- Chromatic aberration: All wavelengths of light cannot be focused in the same position by the lens. Longitudinal chromatic aberration and transverse (or lateral) chromatic aberration are two types of chromatic aberrations that occur not only on axis but also off axis as a feature of field angle (Gennaro et al. 2016).

## 3. Human Eye Image Analysis Criteria

### 3.1. The optical transfer function (OTF)

The optical transfer function as shown in equation (1) consists of two components; they are the modulation transfer function (MTF) which is responsible for the reduction in image modulation or contrast (Manson et al. 2017), and the phase transfer function (PTF) which is responsible for the lateral shifting of the pattern (Devi and Reddy 2018).

$$OTF(V) = MTF(v) \exp \exp (-i PTF(v)) \quad (1)$$

where

$$MTF(v) = \sqrt{v^2(v) + w^2(v)} \quad (2)$$

and

$$PTF(V) = \left[ \frac{w(v)}{V(v)} \right] \quad (3)$$

where

$$v(v) = \frac{\int_{-\infty}^{\infty} h(x)\cos(2\pi vx)dx}{\int_{-\infty}^{\infty} h(x)dx} \quad (4)$$

and

$$w(v) = \frac{\int_{-\infty}^{\infty} h(x) \sin(2\pi vx) dx}{\int_{-\infty}^{\infty} h(x) dx} \quad (5)$$

Where  $v(v)$  is the real part and  $w(v)$  is the imaginary part of the Optical Transfer Function.

### 3.2. Root Mean Square (RMS)

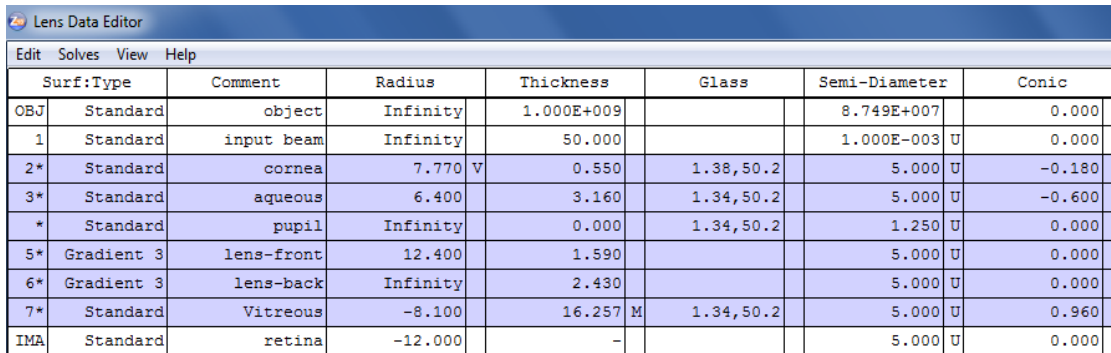
The effect of aberrations on image quality can be visualized using a spot diagram (Kozhevnikov 2017). Another measure of quality that is realized on the spot diagram is the RMS spot radius (Geary 2002). The RMS spot radius is defined as:

$$RMS = \sqrt{\frac{\sum_i [(x_i+x_c)^2 + (y_i+y_c)^2]}{n}} \quad (6)$$

## 4. Analytical Work

To study the impact of the field of view (F.O.V.) and pupil size with different values in the visible region on monochromatic and polychromatic aberrations; the ZEMAX (version 14) optical modeling computer software was used to create Liou and Brennan's 1997 eye model. This model uses the cornea and crystalline lens together as a single element to converge the light beam and focuses it onto the retina (Al-Hamdani 2020).

For constructing the Liou and Brennan eye model, seven surfaces inserted to the model, which are input beam, pupil aperture, cornea, the front portion of the lens, the lens rear portion, aqueous humour, and finally the eye's vitreous body. All these surfaces were inserted between the object and retina surfaces each one with its parameters were entered into the ZEMAX software as seen in Figure (2). As the field of view was set at 5 degrees, the Semi-Diameter values were chosen with values of 1.25, 1.5, 2, 3, 4 and 5 mm. For each of the cases described above, the modulation transfers function (MTF) (which is the magnitude response of the optical system with various spatial frequencies (Bass et al. 2009), (Jiang et al. 2019)) was obtained. Also the *wavefront* aberration coefficients and the spot diagrams root mean square (RMS) were evaluated for all fields of view and pupil Semi-Diameters for both monochromatic light.



Surf	Type	Comment	Radius	Thickness	Glass	Semi-Diameter	Conic
OBJ	Standard	object	Infinity	1.000E+009		8.749E+007	0.000
1	Standard	input beam	Infinity	50.000		1.000E-003	U 0.000
2*	Standard	cornea	7.770	V 0.550	1.38, 50.2	5.000	U -0.180
3*	Standard	aqueous	6.400	3.160	1.34, 50.2	5.000	U -0.600
*	Standard	pupil	Infinity	0.000	1.34, 50.2	1.250	U 0.000
5*	Gradient 3	lens-front	12.400	1.590		5.000	U 0.000
6*	Gradient 3	lens-back	Infinity	2.430		5.000	U 0.000
7*	Standard	Vitreous	-8.100	16.257	M 1.34, 50.2	5.000	U 0.960
IMA	Standard	retina	-12.000	-		5.000	U 0.000

Figure 2. Liou and Brennan 1997 Eye Model Constructed by Using ZEMAX (version 14).

## 5. Results and Analysis

### 5.1. MTF and RMS analysis

Liou and Brennan model was used and analyzed by using different criteria, modulation transfer function (MTF), spot radius on the retina and wavefront aberration coefficients. The effect of eye iris size (Semi-Diameter), entrance pupil diameter E.P.D., and the retina image's responses are studied in detail. Also the effects of E.P.D. on each of the Seidel aberrations were evaluated at 555 nm. MTF curves presented in case of Figure (3) and that illustrated in Equation (2), indicate that the MTF for pupil diameters (1.25 mm) represents the diameter of the diffraction limited optical system. Also MTF was decreased because of the distortion aberration.

RMS differences were studied for a better understanding of retinal image performance beneath the difference of pupil size and the affixed field of view in monochromatic light (555 nm). The pupil uses RMS plot ( $\mu\text{m}$ ) as a function for the size of pupil (1.25, 1.5, 2, 3, 4 and 5 mm), at 5 degrees field of view values. As seen in Figure (4), the values of RMS increased as the pupil size increased at a particular F.O.V.

RMS values of spot diagrams calculated from Equation (6), give an indication about the amount of aberration and its kind, in compare with MTF curves; the highest amount of aberrations appear when the spot size is large (RMS value is high) and this is clear when the pupil Semi-Diameter  $\geq 3$  mm, while the MTF curves provide better image contrast

when MTF has large values ( $\approx 1$ ). Table (2) clears the RMS values of the retinal image according to pupil size variation.

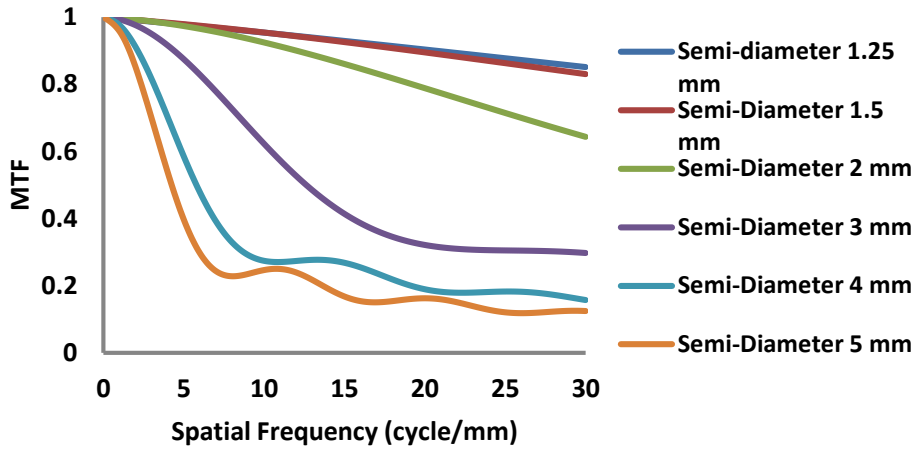


Figure 3. Monochromatic MTF at 5 Degree F.O.V.

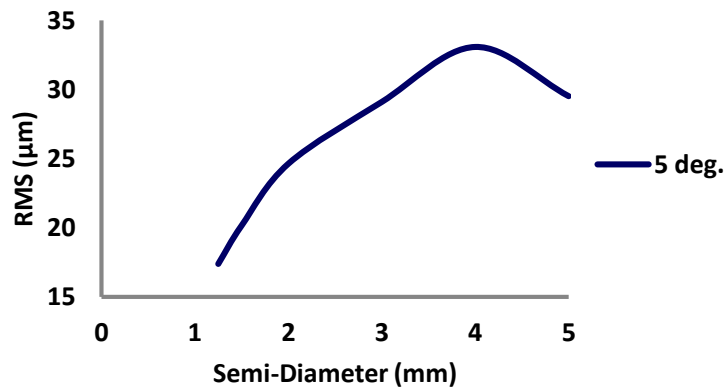


Figure 4. Variation in RMS as Pupil Diameter Changes

Table 2. RMS values of retinal image according to pupil size variation.

Semi-Diameter (mm)	Monochromatic RMS (μm)
1.25	17.382
1.5	20.16
2	24.635
3	29.107
4	33.087
5	29.524

### 5.2. Coefficients of wavefront aberration

The aberration coefficients curves, as seen in Figure (5), will be used to recognize the form of aberration has the greatest impact on MTF deterioration and its effect on the image quality obtained by the human intraocular lens. Because of the spherical aberration ( $W_{040}$ ) generated within the eye, MTF decreased as the Semi-Diameter was increased. As the pupil Semi-Diameter became larger than 1.5 mm, ( $W_{040}$ ) increased, preventing light rays from colliding in the same spot on the retina. Since the rays are on axis and the F.O.V. is set, all types of aberrations are useless in these situations.

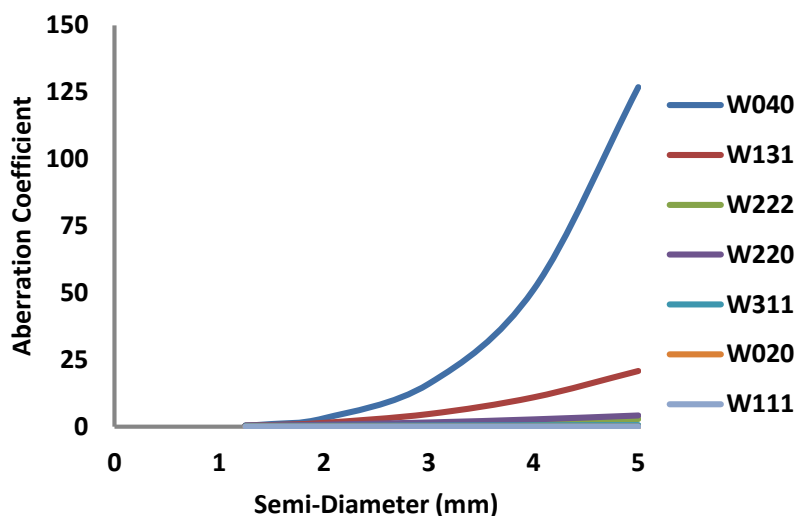


Figure 5: Coefficient of monochromatic wavefront aberration at 5 degree

## 6. Conclusion

This research found that the eye model's performance was at its optimum value when the iris scale (Semi-Diameter) is small (1.25 and 1.5 mm) and the field of view is set to 5 degrees for monochromatic light. When the Semi-Diameter was increased, MTF decreased because the amount of aberrations generated within the eye, affecting image quality. Furthermore, one can deduce that spherical and distortion aberrations are responses to the image quality loss that occurs as EPD increases. All of the findings, which include: MTF, RMS, and wavefront aberration coefficients, one may state that the lower E.P.D. less than 4 represents the situation of close diffraction limited (perfect eye system) at  $EPD \leq 1.25$  mm and  $FOV \leq 5$  degree.

## References

1. Al-Hamdani, A. H. (2020). Improving quality of image vision using aspherical polysulfones contact lens. *AIP Conference Proceedings*, 2213(March). <https://doi.org/10.1063/5.0000260>.
2. Artal, Pablo. (2015). "Image Formation in the Living Human Eye." *Annual Review of Vision Science* 1(1): 1–17.
3. Atchison, D. A., & Thibos, L. N. (2016). Optical models of the human eye. *Clinical and Experimental Optometry*, 99(2), 99–106. <https://doi.org/10.1111/cxo.12352>.
4. Bartuzel, Maciej M., D. Robert Iskander, Iván Marín-Franch, and Norberto López-Gil. (2019). "Defocus Vibrations in Optical Systems—Considerations in Reference to the Human Eye." *Journal of the Optical Society of America A* 36(3): 464.
5. Bass, M., DeCusatis, C., Enoch, J., Lakshminarayanan, V., Li, G., MacDonald, C., Mahajan, V., & Stryland, V. E. (2009). *Handbook of Optics, Third Edition Volume I: Geometrical and Physical Optics, Polarized Light, Components and Instruments(set)* (3rd ed.). McGraw-Hill Education.
6. Batres, L., S. Peruzzo, M. Serramito, and G. Carracedo. (2020). "Accommodation Response and Spherical Aberration during Orthokeratology." *Graefe's Archive for Clinical and Experimental Ophthalmology* 258(1): 117–27.
7. Bretschneider, F., & de Weille, J. (2019). Microscopy and Optical Methods in Electrophysiology. *Introduction to Electrophysiological Methods and Instrumentation*, 285–310. <https://doi.org/10.1016/b978-0-12-814210-3.00010-4>
8. Burns, S. A., Elsner, A. E., Sapoznik, K. A., Warner, R. L., & Gast, T. J. (2019). Adaptive optics imaging of the human retina. *Progress in Retinal and Eye Research*, 68(August 2018), 1–30. <https://doi.org/10.1016/j.preteyeres.2018.08.002>.
9. Cholewiak, S. A., Love, G. D., & Banks, M. S. (2018). Creating correct blur and its effect on accommodation. *Journal of Vision*, 18(9), 1. <https://doi.org/10.1167/18.9.1>.

10. Devi, M Kalpana, and T Venkat Reddy. (2018). "Study of Optical Transfer Function in an Optical System with Gaussian Filter." 10(1): 13–21.
11. Geary, J. M. (2002). Introduction to Lens Design: With Practical Zemax Examples. Willmann-Bell.
12. Gennaro, S. D., Roschuk, T., Maier, S., & Oulton, R. F. (2016). Measuring chromatic aberrations in imaging systems using plasmonic nanoparticles. *Optics Letters*, 41(7), 1688. <https://doi.org/10.1364/ol.41.001688>.
13. Jiang, B., Yang, J., Lv, Z., & Song, H. (2019). Wearable Vision Assistance System Based on Binocular Sensors for Visually Impaired Users. *IEEE Internet of Things Journal*, 6(2), 1375–1383. <https://doi.org/10.1109/jiot.2018.2842229>.
14. Kaschke, M., Donnerhacke, K., & Rill, M. S. (2013). *Optical Devices in Ophthalmology and Optometry: Technology, Design Principles and Clinical Applications* (1st ed.). Wiley-VCH.
15. Kozhevnikov, A. V. (2017). Research of the effect of aberrations on image quality in optical systems. *Computer Optics and Nanophotonics*. <https://doi.org/10.18287/1613-0073-2017-1900-117-121>.
16. Mahajan, V. N. (2011). *Aberration Theory Made Simple* (SPIE Tutorial Text Vol. TT93) (Tutorial Texts) (2nd ed.). SPIE Press.
17. Manson, E. N., Bambara, L., Nyaaba, R. A., Amuasi, J. H., Flether, J. J., & Schandorf, C. (2017). Comparison of Modulation Transfer Function Measurements for Assessing the Performance of Imaging Systems . *Medical Physics International Journal*, 5(2), 188–191.
18. Mijs, A., & Novak, J. (2016). Dependence of depth of focus on spherical aberration of optical systems. *Applied Optics*, 55(22), 5931. <https://doi.org/10.1364/ao.55.005931>
19. Nakajima, H. (2015). *Optical Design Using Excel: Practical Calculations for Laser Optical Systems* (1st ed.). Wiley.
20. Polans, J., Jaeken, B., McNabb, R. P., Artal, P., & Izatt, J. A. (2015). Wide-field optical model of the human eye with asymmetrically tilted and decentered lens that reproduces measured ocular aberrations. *Optica*, 2(2), 124. <https://doi.org/10.1364/optica.2.000124>. [1] (Polans et al. 2015).
21. Smith, W. (2007). *Modern Optical Engineering* (4th ed.). McGraw-Hill Education.
22. Vukobratovich, D., & Yoder, P. (2018). *Fundamentals of Optomechanics* (Optical Sciences and Applications of Light) (1st ed.). CRC Press.